

Spatiotemporal evolution characteristics and attribution analysis of hepatitis A in mainland China

Xiaodi Su, Chunxia Qiu, Chunhui Liu

College of Geomatics, Xi 'an University of Science and Technology, Xi 'an, China

Abstract

This study aimed to analyze the epidemiological characteristics and spatiotemporal clustering of hepatitis A in mainland China from 2004 to 2019 and to evaluate the practical impact of integrating hepatitis A vaccines into the Expanded Program on Immunization (EPI). Spatial and temporal autocorrelation and spatiotemporal scanning statistics were used to perform spatial and temporal characterization to quantify the spatial similarity or degree of aggregation of geographic data, and Geographical and Temporal Weighted Regression (GTWR) models were used to reveal spatial and temporal heterogeneity in the relationships between variables to test for spatial and temporal outbreaks of disease and other factors, such as socio-economic factors. Spatially, the incidence rates exhibited a west-high and east-low spatial differentiation, with the High-High (HH) clusters predominantly located in the western regions, maintaining stability but gradually diminishing. Hepatitis A prevalence peaked during the initial

study period (2004-2008) showing significant spatial clustering. However, since the inclusion of hepatitis A vaccine in the immunization program in 2008, the incidence rates of hepatitis A in mainland China significantly decreased demonstrating the positive impact of immunization strategies. In addition to the effects of vaccination, socio-economic factors such as education level, water resources and age groups showed significant associations with hepatitis A incidence rates. Increased vaccine coverage and improved social conditions are crucial for controlling hepatitis A in China.

Introduction

Hepatitis A is a viral liver infection posing a significant challenge to global public health. It is an acute and usually self-limiting liver infection caused by hepatitis A virus (HAV), primarily transmitted through the fecal-oral route and associated with hygiene conditions and population mobility (Fiore, 2004; Cui *et al.*, 2009; WHO, 2017). The global incidence and mortality rates in 2019 were 22,72.1 per 100,000 (95% confidence interval: 2,121.8–2,421.8) and 0.5 per 100,000 (95% CI: 0.4–0.7), respectively. In developing countries, the likelihood of children getting infected with HAV is very high, especially in children under 10 years old, with a serum positivity rate of up to 100% (Van Damme *et al.*, 2003). In the 1990s, hepatitis A had the highest incidence rate among all types of viral hepatitis in China. By the mid-1990s, northern China, characterized by relatively poor sanitation and lagging economic development, had become a highly endemic area for hepatitis A (Wang *et al.*, 2019, 2021). To prevent this infection, the Chinese government approved the first hepatitis A live attenuated vaccine (L-HepA) in 1992. Followed by the inactivated vaccine (I-HepA), licensed in 2002 and introduced as a free children's vaccine in 2008 under the sponsorship of the Chinese Ministry of Health (Cui *et al.*, 2014, Zhang, 2020).

Geographical Information Systems (GIS) allows for the visualization and analysis of spatial and temporal disease patterns. In recent years, with technological advancements and integration with modelling methods, the application of GIS in epidemiological research has expanded significantly, offering novel perspectives for analyzing the spatiotemporal distribution of infectious diseases and assisting control strategies (Gomez-Barroso *et al.*, 2012; Stoitsova *et al.*, 2015; Leal *et al.*, 2021a). For example, Zhu *et al.* (2018) visualized the spatial clustering of hepatitis A incidence rates in China highlighting clusters concentrated in the western regions of the country. This research group further analyzed the evolution trend of provincial hepatitis A incidence rates in China using multiple linear regression and spatial autocorrelation methods for the exploration of the spatial, non-stationarity of hepatitis A incidence rates in association with population density

Correspondence: Chunxia Qiu, College of Geomatics, Xi 'an University of Science and Technology, Xi 'an, China.
E-mail: 000358@xust.edu.cn

Key words: hepatitis A; spatiotemporal feature analysis; spatial autocorrelation analysis; spatiotemporal scan statistics; geographical and temporal weighted regression; China

Conflict of interest: the authors declare no potential conflict of interest, and all authors confirm accuracy.

Availability of data and materials: all data generated or analyzed during this study are included in this published article.

Received: 19 June 2024.

Accepted: 15 November 2024.

©Copyright: the Author(s), 2024
Licensee PAGEPress, Italy
Geospatial Health 2024; 19:1323
doi:10.4081/gh.2024.1323

This work is licensed under a Creative Commons Attribution-NonCommercial 4.0 International License (CC BY-NC 4.0).

Publisher's note: all claims expressed in this article are solely those of the authors and do not necessarily represent those of their affiliated organizations, or those of the publisher, the editors and the reviewers. Any product that may be evaluated in this article or claim that may be made by its manufacturer is not guaranteed or endorsed by the publisher.



through Geographically weighted regression (Zhu, 2023). In addition to simple integration of GIS technology with geospatial modeling methods for infectious disease analysis, many scholars focus on combining other analytical methods with GIS to investigate the spatiotemporal distribution of infectious diseases. For example, Zheng *et al.* (2021) estimated the temporal trends of hepatitis A incidence rates in different age groups and provinces in China from 1990 to 2018 using Joinpoint regression analysis and assessed the impact of including vaccination in the EPI from 2007 to 2018 through interrupted time series regression. Wang *et al.* (2017) fitted hepatitis A monthly data using autoregressive integrated moving average (ARIMA) models to predict seasonal hepatitis A trends, while Rezaei *et al.* (2021) established two independent spatiotemporal mixed models (GLMM) to predict the prevalence of hepatitis B among blood donors in Iran, and Jeong *et al.* (2023) used Bayesian Poisson regression models to study the spatiotemporal changes of hepatitis A in Korea.

Several studies have investigated the impact of socioeconomic and epidemiological factors on hepatitis A in different countries. For instance, Tapia-Conyer *et al.* (1999) indicated a significant reduction in the HAV rate in Brazil, Argentina and Mexico under moderate to high socioeconomic conditions. Mantovani *et al.* (2015) found poorer socioeconomic conditions in high-incidence areas of hepatitis A in Brazil emphasizing the need to improve health conditions and water treatment in the western Amazon region of Brazil to reduce outbreaks of infectious diseases. Copado-Villagrana *et al.* (2021) pointed out that HAV infections mainly occur in major metropolitan areas in southern and western Mexico, possibly related to the poor medical services in the most marginalized areas. Shanmugam *et al.* 2021 demonstrated a recent decrease in primary HAV infections in elderly populations in India with improved living conditions. Villar *et al.* (2002) found an increase in HAV infections during the rainy season in Brazil. In Para State, Brazil, there was a positive correlation between monthly cumulative precipitation and HAV incidence (Leal *et al.*, 2021b), while Tosepu (2021) found a strong relationship between HAV and weather changes, especially related to rainfall and floods in several regions including Spain, India, China and Egypt.

Given the high risk of morbidity and mortality associated with hepatitis A, implementing spatiotemporal monitoring and identifying risk factors is crucial for determining targeted interventions, rapid detection, and prioritizing resource allocation (Zhao *et al.*, 2023). This study employed spatial autocorrelation and spatiotemporal scan statistics to analyze the spatiotemporal characteristics of hepatitis A data from 31 provinces in mainland China from 2004 to 2019 covering key epidemiological indicators such as incidence, rates and cumulative number of cases (Qian *et al.*, 2023). Building upon this, the study utilized a Geographical and Temporal Weighted Regression (GTWR) model (Chu *et al.*, 2018) to examine the determinants of disease outbreaks in space and time. The results suggest that the combined use of spatial autocorrelation and spatiotemporal scan statistics in spatiotemporal feature analysis can provide comprehensive information on the spatiotemporal distribution of epidemics. This would aid the formulation of targeted intervention policies at different stages of epidemic development and offer valuable insights for understanding the spread and control of epidemics. Our aim was to demonstrate the applicability and limitations of different analytical tools in studying the spatiotemporal dynamics of disease outbreaks and investigate the spatiotemporal changes of hepatitis A in mainland China and the impact of socioeconomic factors. Following a discussion of the applicability

and effectiveness of spatiotemporal analysis methods for hepatitis A, future prevention and control strategies are outlined.

Materials and Methods

Data sources

The disease data used in this study consisted of annual hepatitis A case information from 31 provinces, autonomous regions, and municipalities in mainland China from 2004 to 2019. These data were sourced from the Chinese Disease Prevention and Control Information System, including indicators such as the number of cases and incidence rates. Other data, such as population birth rates, number of enterprise units, number of hospitals and public transportation, were obtained from the National Bureau of Statistics. Weather-related indicators like precipitation were sourced from the National Meteorological Information Center.

Methodologies applied

Time series analysis displayed the temporal trends of hepatitis A incidence rates (number of new cases per 100,000 people annually) at the national and provincial levels. Box plots were used to present basic statistical data (e.g., median, minimum, upper quartile Q3, and lower quartile Q1) and identify outliers in incidence rates to showcase the overall temporal trends of hepatitis A infection rates. The study period (2004–2019) was divided into three periods: 2004–2008, 2009–2013 and 2014–2019, with tables illustrating the specific incidence rates and growth rates for each provincial unit during them. Additionally, Chi-square linear correlation tests were conducted on the incidence rates to identify units showing significant trends.

The study employed two complementary methods to identify spatial clustering of HAV: spatial autocorrelation analysis (Tang *et al.*, 2016) and retrospective space-time scan analysis (Guerrero-Vadillo *et al.*, 2022). Spatial autocorrelation analysis is primarily used to investigate whether the attribute values on spatial units in a region are correlated with the same attribute values on neighboring spatial units, serving as a method to measure the degree of aggregation and dispersion of attribute values on spatial units (Liu *et al.*, 2013; Xia *et al.*, 2015; Ge *et al.*, 2016), including global spatial autocorrelation analysis and local spatial autocorrelation analysis. Global spatial autocorrelation mainly reflects the spatial distribution characteristics of attribute values across the entire region. By calculating the Global Moran's I (ranging from -1 to 1) and conducting a Z-test on this value, the type of spatial distribution of attribute values is determined to be clustered, random or dispersed (Varga *et al.*, 2015). When $p > 0.05$, the spatial distribution of attribute values is random; when it is lower, the spatial distribution of attribute values is non-random. A Global Moran's I value > 0 and $p < 0.05$ indicate a positive spatial correlation of attribute values, with a larger value of the Global Moran's I indicating a more pronounced clustering effect in the spatial distribution of attribute values; a Global Moran's $I < 0$ and $p < 0.05$ indicate a negative spatial correlation of attribute values, with a smaller value of the Global Moran's I indicating a more pronounced dispersion effect in the spatial distribution of attribute values (Abbas *et al.*, 2015).

Local spatial autocorrelation reflects the spatial distribution characteristics of attribute values in local regions (Li *et al.*, 2023).

In this study, Local Moran's I was used to indicate the spatial autocorrelation of each provincial unit with surrounding units (Pavinati *et al.*, 2023). The range of Local Moran's I is also $[-1, 1]$ and its interpretation is similar to that of Global Moran's I . Local Moran's I is useful for detecting spatial clusters and can thus aid in revealing the spatial change patterns of hepatitis A with respect to each provincial unit. Figure 1 illustrates the spatial distribution map of the epidemic, where each square represents a provincial unit, and colors represent the incidence rates. Local Moran's I can detect four types of clusters, reflecting high-high (HH), high-low (HL), low-low (LL), and low-high (LH) clustering patterns (de Oliveria Sousa *et al.*, 2023).

For both global and local Moran's I , Monte Carlo randomization (99,999 permutations) was used to assess significance, with the null hypothesis being that hepatitis A infection cases in China were distributed completely randomly (de Oliveria Sousa *et al.*, 2023, Owada *et al.*, 2022). Retrospective spatiotemporal scan statistics were based on the discrete Poisson distribution spatiotemporal model using SatScan 9.5 software (<https://www.satscan.org/>). Scan windows for confirmed cases in each of the 31 province-level administrative divisions in China were constructed annually, with the time scale parameter set at the annual level and the spatial scale parameter at 50% of the study area (Sawires *et al.*, 2023). Expected case counts were inferred based on actual confirmed case counts and the total population in each area. The Likelihood Ratio (LLR) log was used as the test statistic based on the actual and expected confirmed case counts inside and outside the scan window. The p -value indicates the probability of observing the sample under the given null hypothesis. This study was used to assess the confidence of the statistical results (An *et al.*, 2020).

Results

Epidemiological trends

Based on the inclusion of hepatitis A vaccine in the immunization program timeline, the study period was divided into three phases: 2004-2008, 2009-2013 and 2014-2019. To analyze the provincial disparities and trends in hepatitis A incidence rates in mainland China from 2004 to 2019, a hierarchical treemap was used to visualize the provincial distribution of hepatitis A incidence rates during the study period. As seen in Figure 2, horizontal comparisons of incidence rates across different regions in the same year and vertical comparisons of incidence rates within the same region across different years were conducted. The horizontal comparison shows that the high incidence areas of hepatitis A are clustered in the north-western region of China, such as Xinjiang, Tibet, Gansu and Qinghai, while most of the eastern provinces show low incidence areas, especially in the cities of Shandong and Tianjin; the results of the longitudinal comparison show that the first study period (2004-2008) is the period of high incidence of hepatitis A. This is consistent with the actual situation in China, where the north-western part of the country is a high-prevalence area for hepatitis A due to poor hygiene conditions and relatively low economic development. After vaccination was introduced into the national immunisation programme in 2008, with free vaccination of children, the incidence of hepatitis A in north-western China decreased significantly in the second study period (2009-2013) and then stabilized in the third study period (2014-2019), which did not show

a decrease in incidence due to changes in education levels and population size in different age groups.

A combination of factors may have influenced the incidence of hepatitis A, which is consistent with the results of the GTWR analysis. Figure 3 illustrates the temporal trends of the incidence rates, with suspected outliers and outliers identified on the graph. It is evident that since 2004, the upper quartile, median, lower quartile and mean hepatitis A incidence rates have significantly decreased. Outliers were predominantly found in western China, with Xinjiang being consistently identified as a suspected or actual outlier since 2005, and Liaoning showing outlier behavior in the final period (2014-2019), which is consistent with the incidence patterns seen in Figure 2. Factors contributing to this include poor dietary and hygiene habits in Xinjiang, due to lifestyle and trade interactions as well as Liaoning's coastal cities facing water pollution leading to hepatitis A virus accumulation in the seafood, which is consumed raw by residents. Therefore, vaccination should be further strengthened in areas with high incidence of hepatitis A (e.g. north-western provinces such as Xinjiang and Tibet), especially targeting mobile populations to ensure comprehensive and effective vaccination coverage to reduce the risk of hepatitis A transmission. In coastal cities, focus on reducing water pollution and promoting the consumption of safe seafood to reduce the risk of infection from uncooked food.

To better understand the temporal trends of hepatitis A, we also calculated the growth trends of hepatitis A incidence rates for each provincial unit across the three periods, as shown in Table 1. Provinces with significant linear trends are highlighted in bold. Overall, there is a declining trend in incidence rates over the years, with most provincial units aligning with this overall trend. However, some provincial units exhibit significant differences in hepatitis A growth rates, with some even showing opposite trends. For instance, Shanxi and Xinjiang saw increases of 21.3% and 39.3% in the incidence rates during the period of 2009-2013, sharply contrasting with the average growth rate of just above 50% for all provincial units. Similarly, Shanghai experienced a 90.7% increase in the third period, which is significantly higher than the average rate of change-36%.

Global spatial autocorrelation

From Table 2, it can be observed that the Global Moran's I values regarding the hepatitis A incidence rates for the years 2004-2015 and 2017-2019 exceeded 0.2 with Z-values greater than 1.96, which indicates statistical significance. Thus there was a strong positive correlation and clustered spatial distribution pattern of hepatitis A incidence rates during these periods. In contrast, the value in 2016 did not exceed 0.2, indicating weak global spatial autocorrelation. Additionally, the Z-value after standard normalization was less than the critical value of 1.96 for a normal distribution at a significance level of $p = 0.05$, which shows that the inter-provincial spatial differences in hepatitis A incidence rates in 2016 were not significant, but instead displaying a random distribution pattern.

Local spatial autocorrelation

Figure 4 illustrates the visual results of the local spatial autocorrelation analysis of hepatitis A incidence rates. However, only units with Local Moran's I at a significance level of $p = 0.05$ or better are displayed on the map. In general, during the first part of the study period (2004-2008), all HH clusters were located in the western regions of China (Tibet Autonomous Region, Qinghai,



Gansu, Sichuan), a clustering pattern that persisted until the early stages of the second part of the study period (2009-2013). The change already started in 2010 when Tibet transitioned out of the HH cluster area into an LH cluster state. Later in the second study period, Tibet reverted to an HH cluster state and in the third (2014-2019), Qinghai moved out of the HH cluster area. Eventually, the North (Inner Mongolia Autonomous Region, Beijing, Tianjin, Hebei, Shanxi), East (Shandong, Jiangsu, Shanghai, Zhejiang, Fujian) and Central (Henan, Hubei, Hunan) China regions all exhibited LL cluster characteristics. By the end of the first part of the study period (2007, 2008), Inner Mongolia showed a trend of moving away from the LL cluster area, something that was completed by the end of the third study period, with the LL cluster area gradually shrinking in the East. The HL clusters appeared more randomly, showing a pattern of change only between 2013 and 2019,

with Shanxi and Liaoning being the two units displaying HL cluster features, while the Tibet Autonomous Region exhibited LH cluster features only in 2010 and 2011.

Scan statistics

The spatiotemporal characteristics based on scan statistics utilized a retrospective space-time scan method to investigate the spatial clustering distribution of HAV-diagnosed cases. The Markov Chain Monte Carlo (MCMC) algorithm was employed to simulate 999 datasets, and the scan window with the highest anomaly level was determined based on the ranking of real data within the simulated datasets and the calculated *p*-values. Unusually high or low disease incidence was detected by scanning spatial and temporal windows of varying sizes and identifying the spatial and temporal

Table 1. Change in the rate of hepatitis A incidence in China over the study period.

Region	2004-2008 Change (%)	Hepatitis A (cases per 100,000) 2009-2013 Change (%)	2014-2019 Change (%)
Beijing	3.07-1.64(-46.8)**	0.92-0.43(-53.8)	0.68-0.51(-24.5)**
Tianjin	1.42-0.43(-69.69)**	0.31-0.26(-16.78)	0.48-0.38(-20.46)**
Hebei	2.83-1.76(-37.67)**	1.13-0.69(-38.78)*	0.85-0.60(-29.71)**
Shanxi	3.60-2.69(-25.25)**	2.14-2.59(21.28)**	3.39-4.00(18.03)*
Neimenggu	5.78-2.70(-53.27)**	2.00-1.20(-39.86)	1.19-0.92(-22.75)**
Liaoning	8.09-4.33(-46.44)**	3.36-2.40(-28.49)	3.89-5.70(46.58)**
Jilin	6.60-1.62(-75.40)**	1.64-0.60(-63.69)**	0.67-0.93(38.80)**
Heilongjiang	5.16-1.22(-76.44)**	1.03-0.59(-43.03)**	0.63-0.71(12.56)**
Shanghai	3.69-1.66(-54.96)**	1.29-0.54(-58.21)	0.82-1.56(90.67)**
Jiangsu	4.76-2.56(-46.23)**	1.83-0.70(-61.87)**	0.85-0.91(7.44)**
Zhejiang	8.51-2.88(-66.16)**	2.11-0.86(-59.11)**	0.93-0.89(-4.17)**
Anhui	5.54-2.55(-53.91)**	1.74-1.33(-23.42)**	1.19-0.82(-31.40)
Fujian	6.15-3.18(-48.28)**	2.99-1.33(-55.65)**	1.44-1.15(-20.08)**
Jiangxi	9.08-4.24(-53.26)**	3.03-0.75(-75.30)**	0.67-0.63(-5.60)**
Shandong	2.15-0.66(-69.16)**	0.55-0.41(-24.33)	0.68-0.48(-29.29)**
Henan	9.18-4.53(-50.61)**	4.28-1.00(-76.58)**	0.79-0.22(-72.09)**
Hubei	5.88-3.66(-37.79)**	3.29-1.67(-49.22)**	1.61-1.41(-12.67)**
Hunan	3.00-2.32(-22.91)	1.96-0.96(-51.22)**	0.97-0.84(-12.90)
Guangdong	2.37-1.84(-22.44)	1.85-1.33(-27.91)	1.52-1.43(-6.36)
Guangxi	4.56-3.65(-20.01)*	2.92-1.42(-51.35)**	1.84-1.60(-13.45)
Hainan	13.60-4.66(-65.70)	2.99-1.25(-58.07)**	1.03-0.71(-31.26)**
Chongqing	12.70-6.75(-46.81)**	5.35-3.02(-43.68)**	3.39-2.30(-32.27)**
Sichuan	11.47-6.26(-45.39)**	5.84-4.19(-28.31)**	3.23-2.26(-30.09)**
Guizhou	16.87-15.79(-6.37)	9.62-1.03(-89.32)**	1.25-0.73(-41.67)**
Yunnan	12.14-11.41(-6.00)*	8.65-2.94(-66.00)**	2.45-1.93(-21.00)**
Xizang	18.34-17.99(-1.90)	14.04-7.89(-43.81)	5.86-2.94(-49.94)
Shaanxi	7.19-3.44(-52.13)**	2.62-1.29(-50.80)**	1.07-0.65(-39.58)**
Gansu	27.55-16.82(-38.95)	12.15-3.22(-73.52)**	2.61-2.82(8.06)**
Qinghai	18.03-15.18(-15.81)	11.71-10.69(-8.66)*	7.37-6.25(-15.23)**
Ningxia	20.60-18.62(-9.60)	17.17-1.42(-91.72)*	2.09-2.14(2.03)**
Xinjiang	20.85-16.04(-23.08)	8.88-12.38(39.34)	26.17-4.23(-83.82)
SUM	9.06-5.91(-35)**	4.50-2.27(-51)**	2.63-1.70(-36)**

Percentages highlighted in bold indicate units exhibiting significant linear trends within the sub-period; *statistically significant at *p*=0.01; **statistically significant at *p*=0.005; ***statistically significant at *p*=0.001.

location and duration of clusters. The results of the retrospective space-time scans are shown in Figure 5. From 2004 to 2019, five hepatitis A cluster categories were identified. The five cluster types (I-V) indicate areas of clustering with different levels of significance or risk, with type I being the main cluster, indicating that the area has a significantly higher than expected incidence of hepatitis A and is likely to be a major hotspot of outbreak transmission. The clusters are arranged in ascending order of risk, so that the other types of clustering are also explained. During the first two study periods (2004-2013), Type I clustering of hepatitis A was concentrated in the western regions of China with Tibet at the center (involving 9 provinces), characterized by a large cluster area and low spatial clustering intensity. Clusters of Type II and Type IV persisted in Henan and Liaoning units, respectively, with small cluster ranges making them indiscernible on the map. Type III clusters were consistently observed in the south-eastern and coastal areas with Jiangxi at the centre indicating high spatial clustering intensity due to their smaller cluster areas.

In the third study period (2014-2019), the spatial cluster areas increased to five categories. The Type I area significantly reduced in size and was only observed in Xinjiang. The western regions of China (excluding Tibet) exhibited Type III clustering, with larger cluster areas, with and reduced spatial clustering intensity compared to the previous two periods. The coastal the area shifting southwards focusing Guangdong as Type IV clustering. Type II and Type V clusters were observed in the Henan and Liaoning units, respectively, with small cluster ranges making them indiscernible on the map. The *p*-values met the criteria, thus these results were deemed reasonable. Table 3 provides more detailed information regarding the results of the space-time scan.

Relevant influencing factors

GTWR was used to quantify the impact of relevant influencing factors from 2004 to 2019 on the hepatitis A incidence rate. This covered 15 factors and the results indicated that 13 significantly influenced the hepatitis A incidence rate, albeit at varying degrees. Education level emerged as a primary factor showing a significant

negative correlation with the incidence rate, suggesting that increased education levels may reduce the incidence rate of hepatitis A. Population numbers in various age groups also exhibited significant impacts on the incidence rate, with a strong positive correlation observed for the population aged 0-14 years, indicating that changes in population numbers across different age groups could affect the transmission pathways and prevalence of hepatitis A. This aligns with the observed outbreak of the disease during 2005-2009, that occurred especially in rural areas in primary and secondary schools, which can explain the surge in incidence rates in remote regions such as Xinjiang, Tibet, and Qinghai as depicted in Figure 5(a) and 5(b). It is recommended that health education for high prevalence areas should be strengthened and basic health knowledge should be promoted, especially in rural areas where educational resources are weak, to raise awareness of hepatitis A prevention and control.

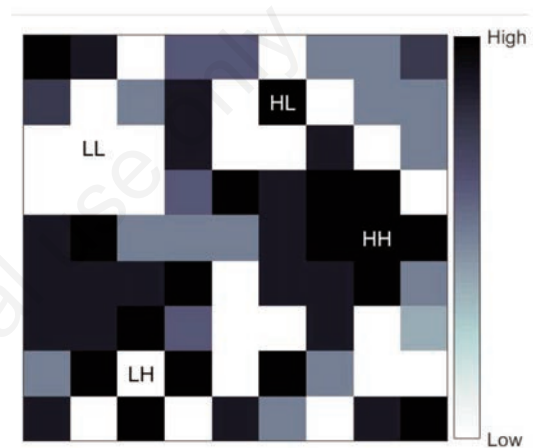


Figure 1. Four types of spatial clusters detected by local Moran's I. HH, high-high; HL, high-low; LH, low-high; LL, low-low.

Table 2. Spatiotemporal clustering of hepatitis A epidemic in mainland China based on global spatial autocorrelation.

Year	Moran's <i>I</i>	Z	p	Spatial pattern
2004	0.4823	5.8991	<0.05	Clustered
2005	0.3952	5.3303	<0.05	Clustered
2006	0.4297	5.4897	<0.05	Clustered
2007	0.2843	3.8781	<0.05	Clustered
2008	0.5501	6.6170	<0.05	Clustered
2009	0.5065	6.2580	<0.05	Clustered
2010	0.2008	3.4510	<0.05	Clustered
2011	0.3052	4.1803	<0.05	Clustered
2012	0.5521	7.2940	<0.05	Clustered
2013	0.6196	8.2661	<0.05	Clustered
2014	0.2476	6.3364	<0.05	Clustered
2015	0.5306	8.6785	<0.05	Clustered
2016	0.0851	1.9001	<0.05	Clustered
2017	0.3096	4.4891	<0.05	Clustered
2018	0.4995	6.4041	<0.05	Clustered
2019	0.2191	2.9825	<0.05	Clustered

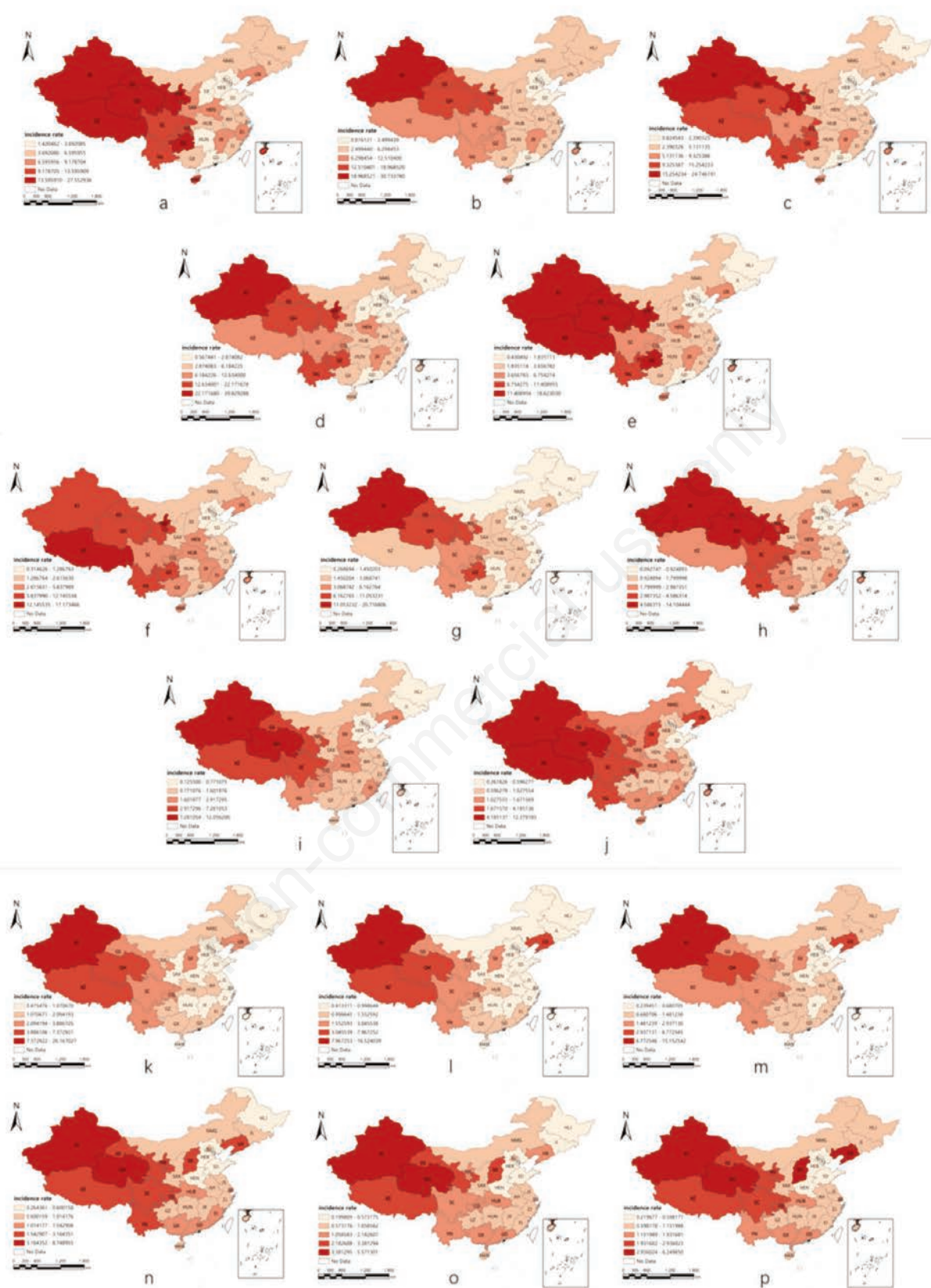


Figure 2. Spatiotemporal clustering of hepatitis in mainland China 2004-2019.

Furthermore, the urban water supply rate showed a significant negative correlation with the incidence rate of hepatitis A, suggesting that widespread urban water supply may reduce its transmission. This explains the persistently high incidence rates and case numbers in Xinjiang compared to other regions as shown in Figures 5(c) and 5(d). In the third study period of this research, mainland China had universally implemented the hepatitis A vaccine, which has led to a significant decrease in incidence rates in other regions compared to the first two study periods. However, Xinjiang, located in an inland arid region with relatively scarce water resources, faced challenges, such as substandard drinking water quality or insufficient water supply, increasing the risk of transmission of waterborne this type of infectious diseases. Therefore, the government should prioritize improving water supply conditions in remote and arid areas to ensure safe water for residents and reduce the incidence of water-borne diseases. In addition, factors such as disposable income, number of hospitals and rail transport, while having a relatively small impact on the incidence of hepatitis A, still showed some degree of correlation indicating their importance in influencing the incidence of

the disease. For example, increasing healthcare resources in remote areas could improve early detection and control of disease, thereby helping to manage and prevent hepatitis A outbreaks. In addition, the expansion of rail transport may affect the frequency of population movements suggesting the need to strengthen hepatitis A prevention measures at transport hubs.

Discussion

This paper, analyzed the spread of hepatitis A to provide a scientific basis for future responses to similar major public health events by combining temporal analysis methods with a geographical perspective. We discussed two methods, namely spatial autocorrelation analysis and retrospective space-time scan statistics, and their application to the spatiotemporal development of hepatitis A epidemic in China from 2004 to 2019, spanning 16 years. The results revealed four main spatial clusters: i) the Huaxi region, primarily Tibet, Qinghai, etc.; ii) the Huazhong region, mainly Henan; iii) the southeastern coastal region, mainly Fujian, Jiangxi;

Table 3. Analysis of temporal and spatial aggregation of confirmed hepatitis A cases in mainland China 2004-2019.

Year	Time (Year)	Cluster type	Coordinates and radius	Population	Location (ID below)	Cases (No.)	RR	LLR	p
2004-2008	2006-2007	1	29.646222N 91.122398E 1,700.26 km	251,805,096	XZ, SC, QH YN,GS, CQ, GZ, XJ, NX	73,920	2.98	2,8045.111693	<0.001
	2004	2	34.743303N 113.640689E	0 km	94,554,732	HEN	8896	1.63	893.532133
	2004	3	26.128575N 119.290632E	469.76 km	129,961,880	FJ, JX, XJ	10100	1.40	506.136932
	2004	4	41.740251N 123.473718E	0 km	42,644,776	LN	3369	1.41	174.644224
2009-2013	2009-2010	1	29.646222N 91.122398E 1,700.26 km	254,216,596	XZ, SC, QH, YN, GS, CQ, SC, XJ, NX	40454	4.24	2,4034.094221	<0.001
	2009	2	34.743303N 113.640689E	0 km	94,197,267	HEN	4036	1.84	605.011458
	2009	3	28.709753N 115.848365E 265.98 km	102,385,531	JX, HUB	3213	1.36	132.712071	
	2009	4	41.740251N 123.473718E	0 km	43,756,459	LN	1449	1.43	80.654391
2014-2019	2014-2016	1	43.921532N 87.590117E 0 km	24,409,906	XJ	13299	13.95	2,2048.653138	<0.001
	2014-2016	2	41.740251N 123.473718E	0 km	43,299,331	LN	6625	3.52	3507.854230
	2014-2016	3	36.080212N 103.818506E 802.61 km	226,094,131	GS, QH, NX, SAX, SC, CQ, SX	17779	1.89	2,664.929947	
	2014	4	23.190597N 113.235948E 501.58 km	17,5715,639	GD, HAN, GX	2585	1.06	4.007620	0.827
	2014	5	30.669442N 114.266197E 0 km	58,835,691	HUB	936	1.08	2.644523	0.996

RR, Relative risk; LLR, Log-likelihood ratio; BJ, Beijing, TJ, Tianjin, HEB, Hebei, SX, Shanxi, NMG, Neimenggu, LN, Liaoning, JL, Jilin, HLJ, Heilongjiang, SH, Shanghai, JS, Jiangsu, ZJ, Zhejiang, AH, Anhui, FJ, Fujian, JX, Jiangxi, SD, Shandong, HEN, Henan, HUB, Hubei, HUN, Hunan, GD, Guangdong, GX, Guangxi, HAN, Hainan, CQ, Chongqing, SC, Sichuan, GZ, Guizhou, YN, Yunnan, XZ, Xizang, SAX, Shaanxi, GS, Gansu, QH, Qinghai, NX, Ningxia, XJ, Xinjiang.



iv) the northeastern region, mainly Liaoning. Temporally, from 2004-2008, the hepatitis A epidemic situation improved with the enhancement of the social environment and nationwide popularity of vaccines resulting in a gradual decrease in incidence rates but still at high levels. During this period, hepatitis A spread widely in China, showing multiple clusters. By the end of the study, particularly in 2014, the hepatitis A epidemic significantly alleviated, with incidence rates fluctuating within a small range thereafter. This study conducted spatiotemporal epidemiological analysis of HAV to provide a basis for targeted prevention and control strategies in mainland China. Comparing the results, it is evident that each of the two methods applied has its own strengths and limitations when applied to spatiotemporal analysis of hepatitis A. The spatial autocorrelation analysis targeting neighbouring geographic units not only indicates the degree of uneven distribution of incidence rates, but also identifies various types of spatial clusters based on spatial weight matrices (Hu et al., 2014). While this approach is limited to a specific time points, retrospective space-time scan statistics provide a supplement by effectively utilizing time and spatial information. However, the latter analysis is heavily influenced by the provided geographic data and can only identify limited types of spatial clusters (Oviedo et al., 2009). As shown in this study, during the first two study periods (2004-2013), Henan and Liaoning units exhibited spatial clustering, making it challenging to accurately visualize this situation spatially due to the small cluster ranges. Based on the strengths and weaknesses of various spatiotemporal analysis methods and their applications in the HAV transmission, we can summarize their applicability and effectiveness. Spatial autocorrelation analysis is suitable for the early and stable stages of hepatitis A transmission. In the early stage of hepatitis A transmission, this approach can assess the spatial clustering and transmission trends of the epidemic, aiding in identifying the transmission patterns and cluster areas. In the stable stage of the epidemic, spatial autocorrelation analysis assists the understanding

of the ongoing spread of the epidemic, evaluates the interactions between different regions and provides guidance for targeted interventions. Retrospective space-time scan analysis is applicable during the outbreak and following cluster formation. During the former period, retrospective space-time scan analysis helps identify cluster areas and periods of the epidemic, as well as potential sources, guiding the prioritization and scope of epidemic control and prevention measures. In the latter, retrospective space-time scan analysis assists in monitoring the spread and evolution trends of hepatitis A, promptly identifying new cluster areas and providing timely decision-making support for epidemic control.

Overall, the reported cases from all provincial units indicate that China still faces a significant threat from hepatitis A, with Global Moran's *I* incidence rate reaching the significant level of 0.05 in this study stage demonstrating spatial concentration of reported cases. This aligns with previous research on the distribution of this infection and reveals different spatial variation patterns at different times and locations. From 2004 to 2019, there was a decreasing trend in the incidence rate, with HH cluster areas remaining relatively stable but gradually shrinking. In the first study period (2004-2008), all HH cluster areas were located in western China, while only Qinghai had completely moved out of the this area by the end of the third study period in 2019. Space-time scan analysis highlighted the severe prevalence of hepatitis A in the western regions. This prevalence pattern can be attributed to two main factors: firstly, large-scale hepatitis A vaccination campaigns were conducted in the 1990s. Both the live attenuated and the inactivated hepatitis A vaccines were included in the national immunization program as Class A vaccines (the national immunization program defines Class A vaccines as those being mandatory for all citizens and provided free of charge, while Class B vaccines are defined as optional, with people pay for them on a voluntarily basis); secondly, hepatitis A is a fecal-oral transmitted hepatitis, and the relatively underdeveloped economy of the western

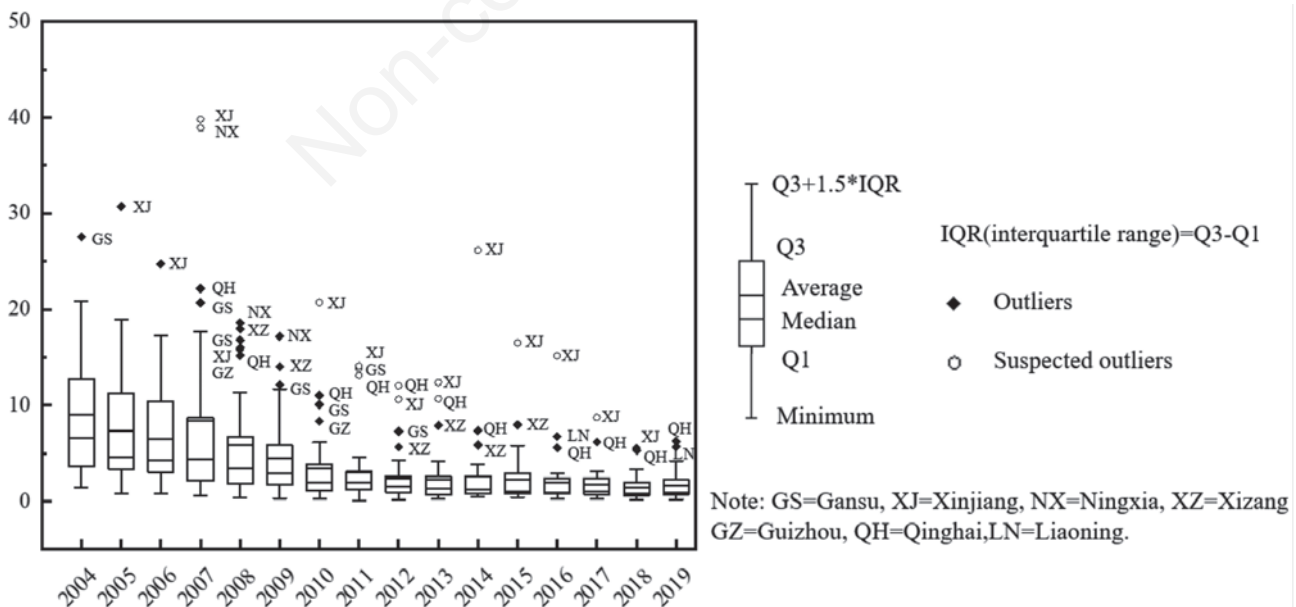


Figure 3. The temporal trends of hepatitis A incidence rates during the study period.

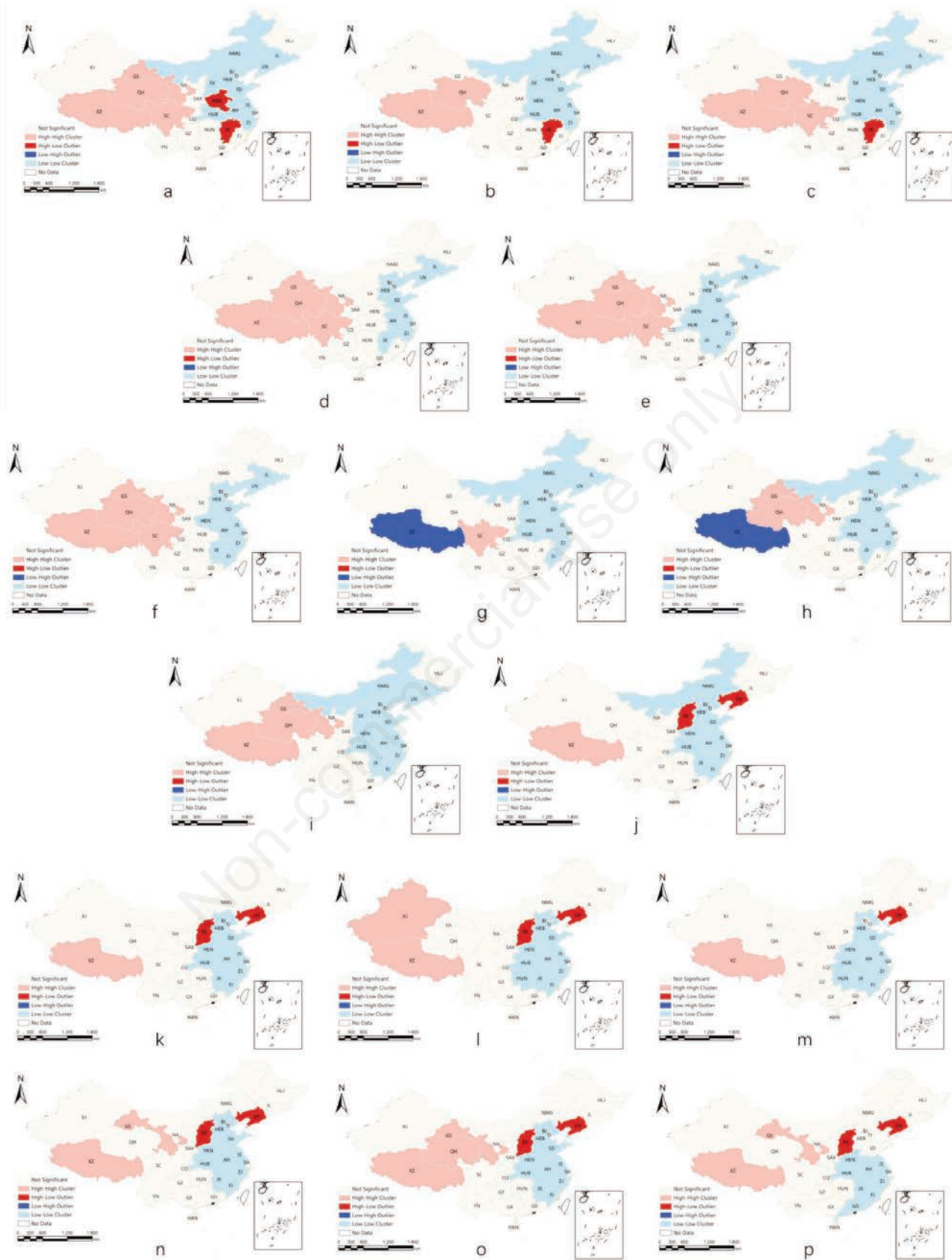


Figure 4. The spatiotemporal clustering of hepatitis A in mainland China based on local autocorrelation

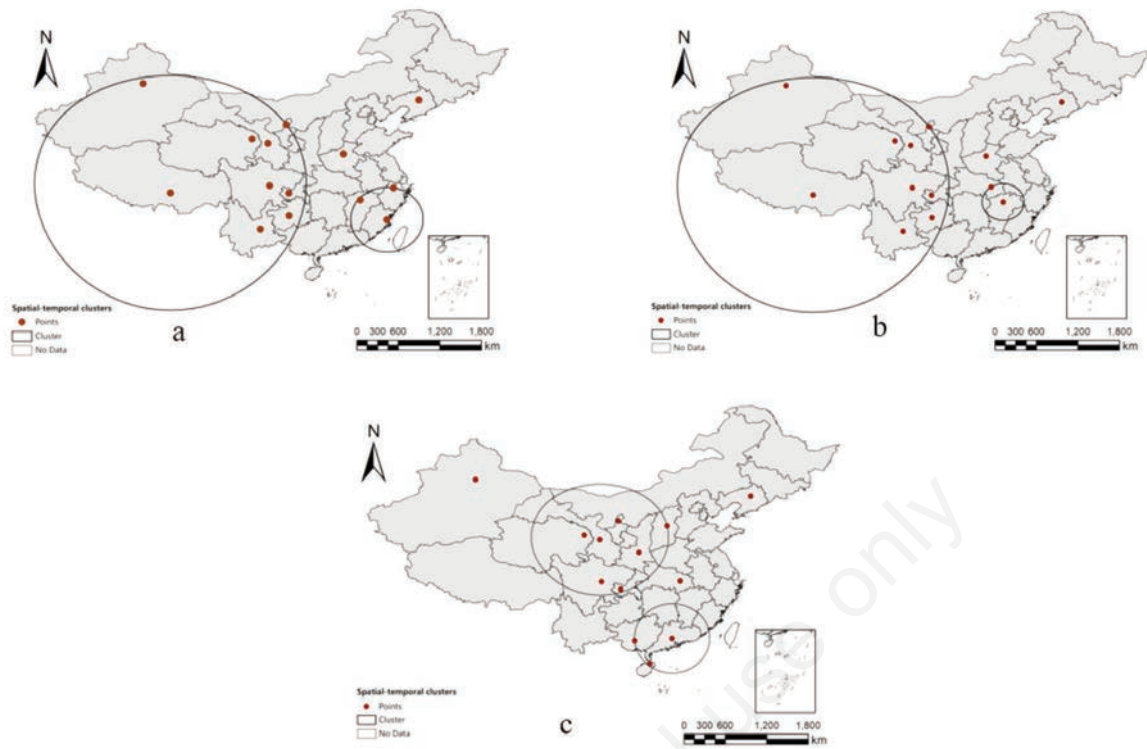


Figure 5. Spatiotemporal clustering of the population diagnosed with hepatitis A in mainland China based on space-time scan.

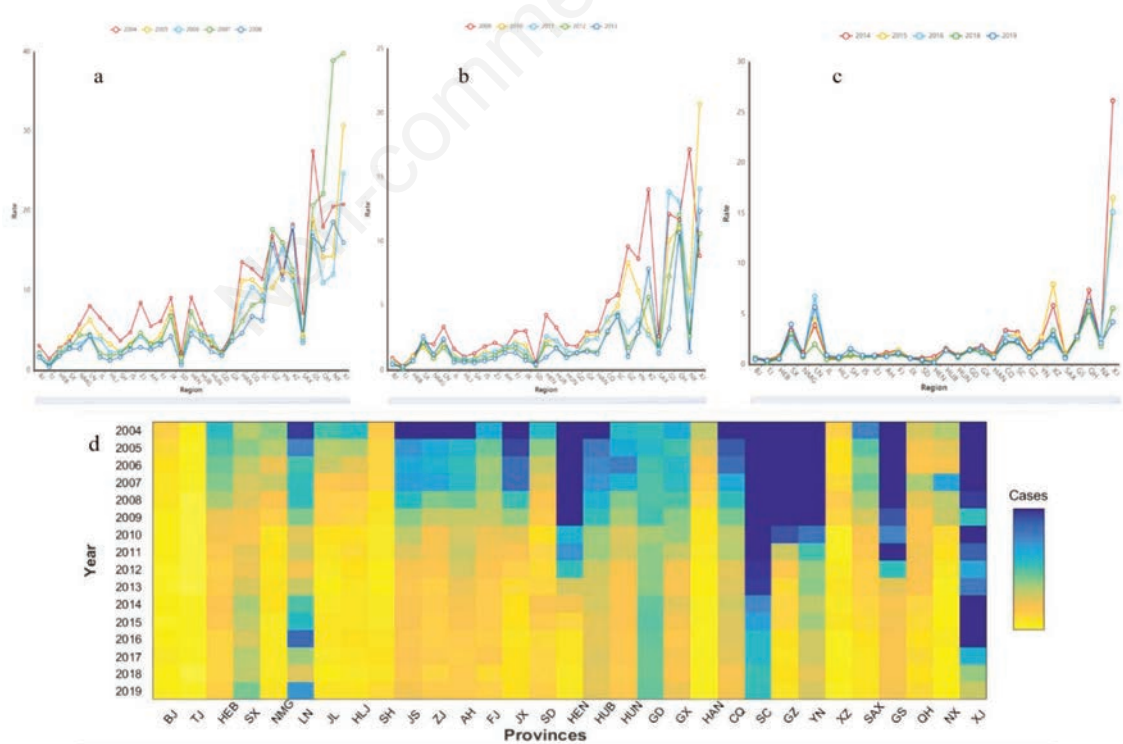


Figure 6. Hepatitis A infection rates in the province-level administrative divisions of mainland China over the study period. Panel a to c show the annual incidence rate changes over the three periods of the study; panel d shows annual number of cases over the entire study period.

region, with its harsh living environment, faces more difficulties in ensuring food and water security, which explains why the HH areas were remained longer in this region. Based on the above, the following public health strategy recommendations were made to guide resource allocation and risk assessment: the less developed, high-prevalence areas in the West should be given priority to allocating resources for vaccines, especially for vulnerable groups, with increasing sentinel vaccination services to ensure vaccination coverage; secondly, water and food safety measures should be strengthened by promoting safe drinking water projects and health education to reduce the risk of transmission. In addition, it was recommended that a dynamic disease surveillance system be established to track changes in cases in real time through spatial and temporal analysis, and that a risk alert system be established in high-prevalence areas to improve response efficiency; thirdly, long-term, investment should be made in the construction of sanitation facilities in the western region to improve living conditions and reduce the risk of infection through the faecal-oral route of transmission. Finally, China's healthcare conditions have significantly improved, breaking the contamination cycle of hepatitis A, which also helps explain the yearly decrease its incidence rate.

Conclusions

Under incomplete geographical data and precision, appropriate spatiotemporal analysis methods or a combination of multiple methods and technologies can be selected based on different stages of epidemic development, research purposes, and societal conditions to comprehensively understand and evaluate the spatial distribution and transmission characteristics of hepatitis A virus, thereby obtaining more comprehensive and accurate spatiotemporal distribution information of the epidemic to formulate corresponding prevention and control strategies. This information provides the scientific basis for public health policy-making, resource allocation, and epidemic prevention and control, holding significant reference value for future similar public health events. However, the prevention and control of viral hepatitis A in China still requires long-term efforts. Due to the different epidemiological trends in different provinces, it is impossible to develop a unified prevention and control programme. To respond effectively to the hepatitis A epidemic, measures should be adapted to the characteristics of the spatial and temporal distribution of the virus and the situation in each province. At the same time, the government needs to strengthen coordination in the health, food safety and insurance sectors to improve the synergy of interventions. Locally

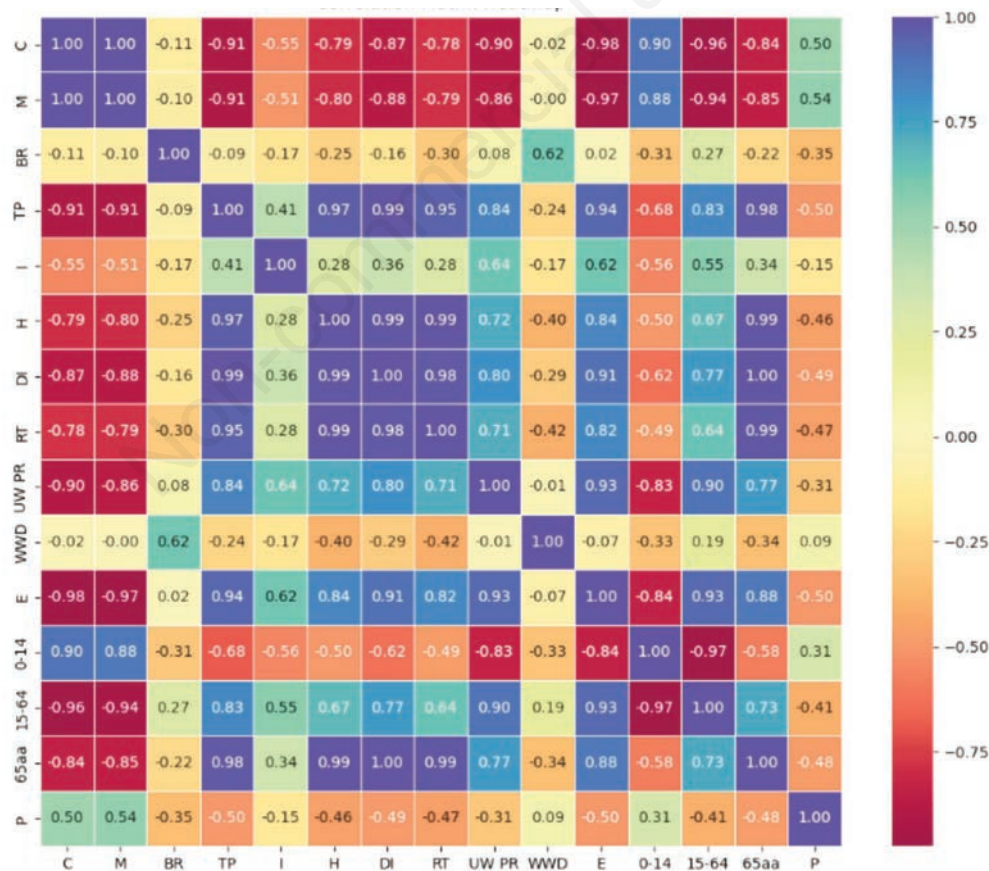


Figure 7. Correlation coefficients of factors influencing the incidence of hepatitis A. C, case count; M, morbidity; BR, birth rate (%); TP, total population (divided by 10,000); I, industries; H, hospitals; DI, disposable income (USD); RT, rail transport(vehicles); UWPR, urban water penetration rate (%); WWD, wastewater discharge (tonnes); E, education; 0-14, population aged 0-14 years (divided by 10,000); 15-64, population aged 15-64 (divided by 10,000); 65aa, population aged ≥ 65 years and over (divided by 10,000); P, precipitation (mm).



tailored prevention and control strategies can help to address regional disparities, thereby enhancing the overall prevention and control effect.

References

- Abbas T, Younus M, Muhammad SA, 2015. Spatial cluster analysis of human cases of Crimean Congo hemorrhagic fever reported in Pakistan. *Infect Dis Poverty* 4(9).
- An J, Zhang XS, Liang XF, 2020. Spatio-temporal clustering of hepatitis A in Gansu province, 2004-2018. *Zhonghua Liu Xing Bing Xue Za Zhi* 41:1319-23.
- Chu HJ, Kong SJ, Chang CH, 2018. Spatio-temporal water quality mapping from satellite images using geographically and temporally weighted regression. *Int J Appl Earth Obs Geoinf* 65:1-11.
- Copado-Villagrana ED, Anaya-Covarrubias JY, Viera-Segura O, 2021. Spatial and temporal distribution of hepatitis A virus and hepatitis E virus among children with acute hepatitis in Mexico. *Viral Immunol* 34:653-7.
- Cui F, Hadler SC, Zheng H, 2009. Hepatitis A surveillance and vaccine use in China from 1990 through 2007. *J Epidemiol* 19:189-95.
- Cui F, Liang X, Wang F, 2014. Development, Production, and Postmarketing Surveillance of Hepatitis A Vaccines in China. *J Epidemiol* 24:169-77.
- de Oliveria Sousa LF, de Sousa Santos ER, Oliveira RM, Batalha Andrade RL, Calazans Batista JF, Oliveira Lima S, 2023. Hepatitis mortality in Brazil and regions, 2001-2020: temporal trend and spatial analysis. *Rev Bras Epidemiol* 26:e230029.
- Fiore AE, 2004. Hepatitis A transmitted by food. *Clin Infect Dis* 38:705-15.
- Ge E, Zhang X, Wang X, 2016. Spatial and temporal analysis of tuberculosis in Zhejiang Province, China, 2009-2012. *Infect Dis Poverty* 5(11).
- Gomez-Barroso D, Varela C, Ramis R, 2012. Space-time pattern of hepatitis A in Spain, 1997-2007. *Epidemiol Infect* 140:407-16.
- Guerrero-Vadillo M, Penuelas M, Dominguez A, 2022. Epidemiological Characteristics and Spatio-Temporal Distribution of Hepatitis A in Spain in the Context of the 2016/2017 European Outbreak. *Int J Environ Res Public Health* 19:16775.
- Hu Y, Xiong C, Zhang Z, 2014. Changing Patterns of Spatial Clustering of Schistosomiasis in Southwest China between 1999-2001 and 2007-2008: Assessing Progress toward Eradication after the World Bank Loan Project. *Int J Environ Res Public Health* 11:701-12.
- Jeong J, Kim M, Choi J, 2023. Investigating the spatio-temporal variation of hepatitis A in Korea using a Bayesian model. *Front Public Health* 10:1085077.
- Leal PR, De Paula RJ, Guimarães S, 2021a. Sociodemographic and spatiotemporal profiles of hepatitis-A in the state of Pará, Brazil, based on reported notified cases. *Geospat Health* 16:981.
- Leal PR, Souza E, Guimaraes RJDP, Kampel M, 2021b. Associations Between Environmental and Sociodemographic Data and Hepatitis-A Transmission in Pará State (Brazil). *Geohealth* 5:e2020GH000327.
- Li J, Xu Z, Zhu H, 2023. Spatial-temporal analysis and spatial drivers of hepatitis-related deaths in 183 countries, 2000-2019. *Sci Rep* 13:19845.
- Liu Y, Wang X, Liu Y, 2013. Detecting spatial-temporal clusters of HFMD from 2007 to 2011 in Shandong Province, China. *PLoS One* 8:e63447-e63447.
- Mantovani SA, Delfino BM, Martins AC, 2015. Socioeconomic inequities and hepatitis A virus infection in Western Brazilian Amazonian children: spatial distribution and associated factors. *BMC Infect Dis* 15:1-12.
- Oviedo M, Munoz P, Dominguez A, 2009. Evaluation of mass vaccination programmes: the experience of Hepatitis A in Catalonia. *Rev Esp Salud Publica* 83:697-709.
- Owada K, Sarkar J, Rahman MK, 2022. Epidemiological Profile of a Human Hepatitis E Virus Outbreak in 2018, Chattogram, Bangladesh. *Trop Med Infect Dis* 7:170.
- Pavinati G, de Lima LV, Palmieri IGS, Magnabosco GT, 2023. Distribution and spatial autocorrelation of viral hepatitis B and C in Parana, Brazil: an ecological study, 2011-2019. *Epidemiol Serv Saude* 32:e2022888.
- Qian J, Yue M, Huang P, Ai L, Zhu C, Wang C, Luo Y, Yue N, Wu Y, Zhang Y, Wang C, Tan W, 2023. Spatiotemporal heterogeneity and impact factors of hepatitis B and C in China from 2010 to 2018: Bayesian space-time hierarchy model. *Front Cell Infect Microbiol* 13:1115087.
- Rezaei N, Maghsodlu M, Sheidaei A, Kafiabad SA, Gohari K, Zadsar M, Delavari F, Sharifi Z, Yoosefi M, Farzadfar F, Asadi-Lari M, 2021. Spatio-Temporal Analysis of the Hepatitis B Prevalence in Iranian Blood Donors from 2000 to 2016 at National and Provincial Level. *Iran J Public Health* 50:1854-62.
- Sawires R, Osowicki J, Clothier H, 2023. Pediatric Hepatitis and Respiratory Viruses: A Spatiotemporal Ecologic Analysis. *Pediatr Infect Dis Journal* 42:276-80.
- Shanmugam N, Sathyasekaran M, Rela M, 2021. Pediatric Liver Disease in India. *Clin Liver Dis* 18:155-7.
- Stoitsova S, Gomez-Barroso D, Vallejo F, 2015. Spatial analysis of hepatitis a infection and risk factors, associated with higher hepatitis a incidence in Bulgaria: 2003-2013. *Compt Rend Acad Bulg Sci* 68:1071-8.
- Tang L, Zhang Y, Xing D, 2016. Spatial data based study of distribution of hepatitis C in Chongqing. *Zhonghua Liu Xing Bing Xue Za Zhi* 37:80-4.
- Tapia-Conyer R, Santos JI, Cavalcanti AM, 1999. Hepatitis A in Latin America: a changing epidemiologic pattern. *Am J Trop Med Hyg* 61:825-9.
- Tosepu R, 2021. Increased risk of hepatitis a due to weather changes: a review. *IOP Conference Series: Earth and Environmental Science*. IOP Publishing 2021:012085.
- Van Damme P, Banatvala J, Fay O, 2003. Hepatitis A booster vaccination: is there a need? *Lancet* 362:1065-71.
- Varga C, Pearl DL, McEwen SA, Sargeant JM, Pollari F, Guerin MT, 2015. Area-level global and local clustering of human Salmonella Enteritidis infection rates in the city of Toronto, Canada, 2007-2009. *BMC Infect Dis* 15:15:359.
- Villar LM, De Paula VS, Gaspar AMC, 2002. Seasonal variation of hepatitis A virus infection in the city of Rio de Janeiro, Brazil. *Rev Inst Med Trop Sao Paulo* 44:289-92.
- Wang F, Sun X, Wang F, Zheng H, Jia Z, Zhang G, Bi S, Miao N, Zhang S, Cui F, Li L, Wang H, Liang X, Rodewald LE, Feng Z, Yin Z, Shen L, 2021. Changing Epidemiology of Hepatitis A in China: Evidence From Three National Serological Surveys and the National Notifiable Disease Reporting

- System. *Hepatology* 73:1251-60.
- Wang H, Gao P, Chen W, Bai S, Lv M, Ji W, Pang X, Wu J., 2019. Changing epidemiological characteristics of Hepatitis A and waning of Anti-HAV immunity in Beijing, China: a comparison of prevalence from 1990 to 2017. *Hum Vaccin Immunother* 15:420-425.
- Wang S, 2017. Application of temporal distribution modelling in the analysis of hepatitis A epidemic trends. Zhejiang University.
- WHO, 2017. Global Hepatitis Report. Available at <https://www.who.int/publications/i/item/9789241565455>.
- Xia J, Cai S, Zhang H, Lin W, Fan Y, Qiu J, Sun L, Chang B, Zhang Z, Nie S, 2015. Spatial, temporal, and spatiotemporal analysis of malaria in Hubei Province, China from 2004-2011. *Malar J*, 14:145. doi:10.1186/s12936-015-0650-2.
- Zhang L, 2020. Hepatitis A vaccination. *Hum Vaccin Immunother* 16:1565-1573.
- Zhao N, Guo X, Wang L, Zhou H, Gong L, Miao Z, Chen Y, Qin S, Yu Z, Liu S, Wang S, 2023. Changing spatiotemporal patterns for hepatitis of unspecified aetiology in China, 2004-2021: a population-based surveillance study. *Front Public Health*, 11:1177965.
- Zheng B, Wen Z, Pan J, 2021. Epidemiologic trends of hepatitis A in different age groups and regions of China from 1990 to 2018: observational population-based study. *Epidemiology & Infection* 149 e186
- Zhu JJ, Hu DL, Hong XQ, Zha WT, Lü Y, 2018. Analysis of distribution characteristics and prediction model of hepatitis A incidence based on spatiotemporal big data. *Chin J Dis Control Prev* 22:1144-7.
- Zhu Z, 2023. Spatial and temporal evolution of the incidence of hepatitis A among provincial residents in China and analysis of the factors affecting it. Xinjiang University of Finance and Economics; Xinjiang University of Finance and Economics.

Non-commercial use only